Journal of Nuclear Materials 408 (2011) 1–6

Contents lists available at ScienceDirect

Journal of Nuclear Materials

journal homepage: www.elsevier.com/locate/jnucmat

Oxygen ion irradiation effect on corrosion behavior of titanium in nitric acid medium

S. Ningshen [a], U. Kamachi Mudali [b,*], P. Mukherjee [b], P. Barat [b], Baldev Raj [a]

[a] Indira Gandhi Centre for Atomic Research, Kalpakkam 603 102, India
[b] Variable Energy Cyclotron Centre, 1/AF, Bidhannagar, Kolkata 700 064, India

ARTICLE INFO

Article history:
Received 10 February 2010
Accepted 17 October 2010

ABSTRACT

The corrosion assessment and surface layer properties after O^{5+} ion irradiation of commercially pure titanium (CP-Ti) has been studied in 11.5 N HNO_3. CP-Ti specimen was irradiated at different fluences of 1×10^{13}, 1×10^{14} and 1×10^{15} ions/cm^2 below 313 K, using 116 MeV O^{5+} ions source. The corrosion resistance and surface layer were evaluated by using potentiodynamic polarization, electrochemical impedance spectroscopy (EIS), scanning electron microscopy (SEM) and glancing-angle X-ray diffraction (GXRD) methods. The potentiodynamic anodic polarization results of CP-Ti revealed that increased in ion fluence (1×10^{13}–1×10^{15} ions/cm^2) resulted in increased passive current density due to higher anodic dissolution. SEM micrographs and GXRD analysis corroborated these results showing irradiation damage after corrosion test and modified oxide layer by O^{5+} ion irradiation was observed. The EIS studies revealed that the stability and passive film resistance varied depending on the fluence of ion irradiation. The GXRD patterns of O^{5+} ion irradiated CP-Ti revealed the oxides formed are mostly TiO_2, Ti_2O_3 and TiO. In this paper, the effects of O^{5+} ion irradiation on material integrity and corrosion behavior of CP-Ti in nitric acid are described.

1. Introduction

Austenitic stainless steel of type 304L is mainly used as structural materials for equipments handling nitric acid media in nuclear fuel reprocessing plants [1–3]. However, when the oxidizing power of the nitric acid solution increase with increases in concentration (⩽8 N), temperature (⩽353 K) and in presence of oxidizing species (Fe^{4+}, Cr^{6+}, Pu^{6+}), etc. [3–5]; corrosion potential is shifted into more noble direction over passive region and stainless steel (SS) suffered severe intergranular corrosion (IGC) even if the SS is not sensitized [1–3,5,7]. The advanced nitric acid grade (NAG) SS with controlled chemical composition of impurities like S, B, P, etc., and with higher Si, Cr, etc. have also been found to undergo IGC under such aggressive nitric acid conditions [1,2,4–6]. Studies have been carried out to explore valve metals (Ti, Zr, Hf, Nb and Ta) and its alloys (Ti-5%Ta, Ti-5%Ta-1.8%Nb, etc.) as alternate to austenitic SS for use in nitric acid application [1,7–9]. The corrosion resistance of titanium is attributed to the formation of protective and strongly self-adherent oxide film, mainly composed of TiO_2 and suboxides (Ti_2O_3) at the metal surface [1,7,10,13]. Titanium is known to offer outstanding corrosion resistance in wide variety of environments, especially in oxidizing, neutral, inhibited reducing media [9–13] and at concentrations and temperatures where SS undergoes severe uniform and IGC attack [3,11,13,14]. For this reason, titanium is widely used for handling nitric acid in industrial applications over wide range of conditions as heat exchangers, valves, storage tanks, thermometric devices and marine environments [1,8]. CP-Ti is virtually immune to nitric acid corrosion up to 65% at room temperature [1,3,9]. Similarly, under the widely used conditions of reprocessing plants, i.e. within 35–65% of boiling nitric acid, titanium exhibits low corrosion rates [1,6,13]. Unlike the corrosion behavior of many metals and alloys in nitric acid environments, the corrosion resistance of Ti improves as the impurity levels increases, since the dissolved Ti^{4+} ions formed inhibit corrosion. Further, the presence of oxidizing species (Fe^{3+}, Cr^{6+}, Ti^{4+}, Si^{4+}, etc.) and fission products did not affect the corrosion performance of titanium [7,10], as the presence of oxidizing species with higher redox potential exhibits greater inhibiting effect [3,8]. Hence for these reasons, titanium is considered as a good candidate material for containment, evaporator reboilers and as electrode materials in high temperature process streams in radiochemical processes [1–3,6]. However, unalloyed Ti exhibits accelerated dissolution in hot and pure nitric acid and as well as in vapor condensates environments [1,9]. Also, the presence of solute elements and impurities has an important role in corrosion resistance of titanium in nitric acid [1,3,7]. The segregated solute element like iron dissolve in nitric acid is known to make titanium prone to hydrogen attack [1,3,8]. Hence, the applications of a corrosion resistant layer by anodization, thermal oxidation or alloying

* Corresponding author. Tel./fax: +91 44 27480121.
E-mail address: kamachi@igcar.gov.in (U.K. Mudali).

0022-3115/$ - see front matter © 2010 Elsevier B.V. All rights reserved.
doi:10.1016/j.jnucmat.2010.10.015

with refractory metals are the remedies for avoiding above such corrosion problems in a nitric acid [1,12]. In our recent studies, oxygen irradiation in Ti-0.05 Ta-0.02Nb alloy and anodized CP-Ti revealed no any surface damage and marginal increase in corrosion resistance was observed [12]. However, studies related to corrosion issues of CP-Ti and its alloys in highly aggressive nitric acid environments under irradiated condition are limited and hence the present study attempts this aspect.

The reprocessing of the spent fuel by PUREX process involves series of complex chemical processes and nitric acid is the main process medium used [1,3,13]. Moreover, the presence of intense radiation, particularly gamma, and radioactive contamination of surfaces can cause serious corrosion problems [15–19]. This can cause a change in the surface microstructure, change in point defect clusters, increased concentration of impurities at grain boundaries, internal stress, phase changes, dimensions, mechanical and corrosion properties [15–19]. Similarly, in fast breeder fuel reprocessing plants Ti used as electrolytic dissolver vessel is exposed to highly radioactive condition (10^5 to 10^6 rad/h) in presence of severely corrosive (11.5 N) nitric acid [1,15]. Hence a basic understanding of corrosion damage caused in materials and its relation to corrosion resistance is required. In addition, when materials are exposed to reprocessing environment under intense radiation field, stability of the oxide film formed on such alloy is affected both by the environment and high radioactive ambience [16]. Real exposure to radiation is hazardous; also it takes years to obtain the required condition. Moreover, present experiments have not been carried out under proper simulation and measurements conditions. However, the intention of this work is to evaluate the effects of O^{5+} ion irradiation at different ion fluences on material integrity of CP-Ti. Subsequently, the effects of O^{5+} ion irradiation on corrosion behavior of CP-Ti in 11.5 N nitric acid are investigated in this work.

2. Materials and experimental methods

2.1. Sample preparation

CP-Ti specimens (10 mm × 10 mm) cut from a sheet of 3 mm thickness were used for the present investigation. The chemical composition of CP-Ti is given in Table 1. Specimens were polished up to 1000 mesh SiC finish by mechanical polishing. After polishing, all the specimens were ultrasonically cleaned in acetone and subsequently used for oxygen irradiation and electrochemical experiments.

2.2. Oxygen ion irradiation

The polished samples were mounted on aluminium flange and irradiated with 116 MeV O^{5+} ions to induce irradiation damage on the metals surface. The ion irradiation was carried out at the Variable Energy Cyclotron Centre (VECC), Kolkata, India and the irradiation fluence were given in the range of 1×10^{13}, 1×10^{14} and 1×10^{15} ions/cm^2, respectively. The flange used in irradiation was cooled by continuous flow of water. During ions irradiation, the temperature of the sample did not rise above 313 K as measured by thermocouple connected in close proximity of the sample. The details of ion irradiation experiment have been already described elsewhere [12,15].

Table 1
Chemical composition of CP-Ti in wt.%.

Alloy	Fe	O	N	C	H	Ti
CP-Ti	0.041	0.096	0.003	0.015	0.0025	Balance

2.2.1. Grazing angle X-ray diffractometer measurement

The phases present in CP-Ti with and without O^{5+} ion irradiation were determined by using a grazing angle X-ray diffractometer (GXRD) of STOE Powder Diffraction System instrument with CuK_α radiation at 45 kV, 30 mA and 4°(2θ)/min scanning rate at a grazing angle of 4°.

2.2.2. Scanning electron microscope measurement

The morphology of corrosion attack of each specimen with and without O^{5+} ion irradiation was examined before and after the corrosion test using scanning electron microscope (SEM) of ESEM Philips XL-30 model.

2.3. Electrochemical experiments

2.3.1. Potentiodynamic polarization experiments

All the potentiodynamic anodic polarization experiments were carried out at room temperature using the five neck ASTM electrochemical cell consisting of three working electrodes; reference electrode (Ag/AgCl-Saturated), counter electrode (Pt) and working electrode. The Ag/AgCl reference electrode was linked to the electrochemical cell through salt bridge with Luggin capillary. Solartron 1287 Electrochemical Interface was used for conducting the polarization experiments. The electrode potential was anodically scanned at the rate of 10 mV/min from 0.1 V to 3 V. All the electrode potentials were measured against Ag/AgCl (saturated KCl) reference electrode. Two to three sets of polarization tests were conducted for each specimen and all the polarization plots were almost reproducible. The details of the experimental methodology for the above electrochemical measurements have been already described elsewhere [2,12].

2.3.2. Electrochemical impedance measurements

Electrochemical Impedance Spectroscopy (EIS) measurements were carried out using Solartron 1255 Frequency Response Analyzer (FRA) and Solartron 1287 Electrochemical Interface in the frequency range of 0.01 Hz–100 kHz by superimposing an AC voltage of 10 mV amplitude. All the specimens of CP-Ti were prepassivated at 0.8 V versus Ag/AgCl in 11.5 N HNO_3 for 1 h before EIS measurements. The EIS results were interpreted using simple "equivalent circuit" shown in Fig. 1. The circuit description consists of the arrangement of ($[R_s$ (CPE$||R_P)]$ elements, where R_s is the solution resistance, constant phase element (CPE) in parallel connection with R_P which is the polarization resistance at the interface. The characteristic parameters of these elements values are then obtained directly by fitting the experimental impedance curves using Zview Version 2.6 (Scribner Inc.) software.

The CPE was used in the present investigation for obtaining better fitting for experimental data and this also will represent the generalized double layer film capacitance. The impedance expression of CPE is given by [20,21];

$$Z_{CPE} = 1/[T(j\omega)^n] \quad (1)$$

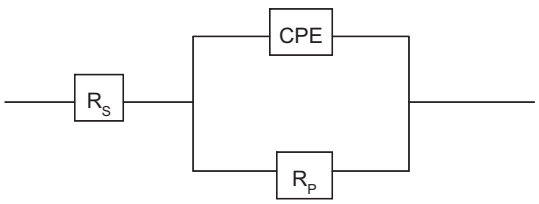

Fig. 1. The equivalent circuit of (R_S[CPE$||R_P$]) used for the fitting of the experimental Nyquist plots.

where ω is the angular frequency, T and n are frequency-independent fit parameters, $j = (-1)^{1/2}$ and $\omega = 2\pi f$, where f is the frequency Hz. n is defined as being [20]:

$$n = 1 - 2\alpha/180 \quad (2)$$

where n is the depression angle (in degrees) that evaluates the semi-circle deformation/depression. The factor n, defined as a CPE power, is an adjustable fitting parameter that lies between 0.5 and 1. When $n = 1$, the CPE describes an ideal capacitor. For $0.5 < n < 1$, the CPE describes a distribution of dielectric relaxation times in frequency space, and when $n = 0.5$ the CPE represents a Warburg impedance [20,21].

All the electrochemical measurement including both potentiodynamic and EIS measurement were carried in aerated and non-stirred condition.

3. Results and discussion

3.1. Phase identification and GXRD pattern

The results of GXRD patterns of CP-Ti specimen with and without O^{5+} ion irradiation at different fluences (1×10^{13}–1×10^{15} ions/cm^2) are shown in Fig. 2a–d. All the GXRD measurement was indexed using the standard Joint Committee for Powder Diffraction Standards (JCPDS) diffraction data. In Fig. 2a–d, the GXRD measurements shows mostly the formation of TiO (32.2°, 38.3°, 53° and 62.9° (JCPDS No: 89–5010)), Ti_2O_3 (23.81°, 40.18°, 72.37° and 86.8° (JCPDS No: 89–4746)) and TiO_2 (35.8°, 38.57°, 40.98°, 54.02° and 83.06° JCPDS No: 89–6975). In unirradiated CP-Ti specimen (Fig. 2a), the reflection peaks observed at 35.1°, 38.4°, 40.1°, 53°, 62.9°, 77.2° and 82.4° (JCPDS No: 05–0682 and 44–1294) correspond to α-Ti or metallic Ti peaks. However, in ion irradiated sample (Fig. 2b–d) decrease in 35.1° and 40.2° peaks and sharp increase in 38.5° peaks were observed. This facet could reveals that the onset of each phase takes place at a specific fluence that can be related to the degree of oxidation of corresponding phases. Moreover, major peak of TiO_2 after oxygen irradiation observed at 27.33° (100%) in Ti-5% Ta-2%Nb alloy in our previous studies were not visible in the present investigation for CP-Ti [12]. Similarly, both the major peaks at 25.28° (100%) for TiO_2 (anatase) and 27.44° (100%) of TiO_2 (rutile) were not observed in this work, thereby indicating that the maximum fluence of O^{5+} ion irradiation used in the present work (1×10^{13}–1×10^{15} ions/cm^2) was not sufficient enough to form high titanium oxidized phase. Hence, this observation might reveal that irradiated oxygen ions are quite minor to enhance oxidation at the surface. Moreover, even under ideal condition several oxide atomic layers are formed at the Ti surface. Thus, the competing process of native oxide layer of the untreated CP-Ti with residual oxygen introduced during irradiation process cannot be ignore, since such competing processes can leads to very broad oxygen distribution with a low oxygen concentration [22,23]. Similarly, in ion irradiated specimens the decrease in 35.8° can be can be interpreted as a reduction of rutile TiO_2 and variation in 40.2° could be associated to reduction of TiO or α-Ti or metallic Ti phase as a result of the increased oxygen fluence. The decrease of 35.8 and 40.2° peaks intensity can also be interpreted to irradiation damage and cold work which can be introduced during sample fabrication or during cutting and polishing that introduces lattice defects and internal stress. The SEM results in Fig. 4c–d indicate the above hypothesis because the morphology of corrosion attack around surrounding matrix is different in each morphology.

3.2. Potentiodynamic polarization results of CP-Ti

The potentiodynamic polarization curves of CP-Ti obtained in 11.5 N HNO_3 with and without ion irradiation are shown in Fig. 3. All the measured polarization parameters such as corrosion potential (E_{Corr}), corrosion current density (I_{Corr}) and passive current density (I_{Pass}) are tabulated and given in Table 2. The E_{Corr} and I_{Corr} values are obtained from the potential current response by extrapolation and curve fitting of Fig. 3. The corrosion potential (E_{Corr}) value obtained under anodic polarization (Fig. 3) corresponds mostly to typical corroding surface. In Fig. 3, the shapes of the potentiodynamic curves are similar but increase in I_{Pass} was observed with increase in irradiation fluence. However, no

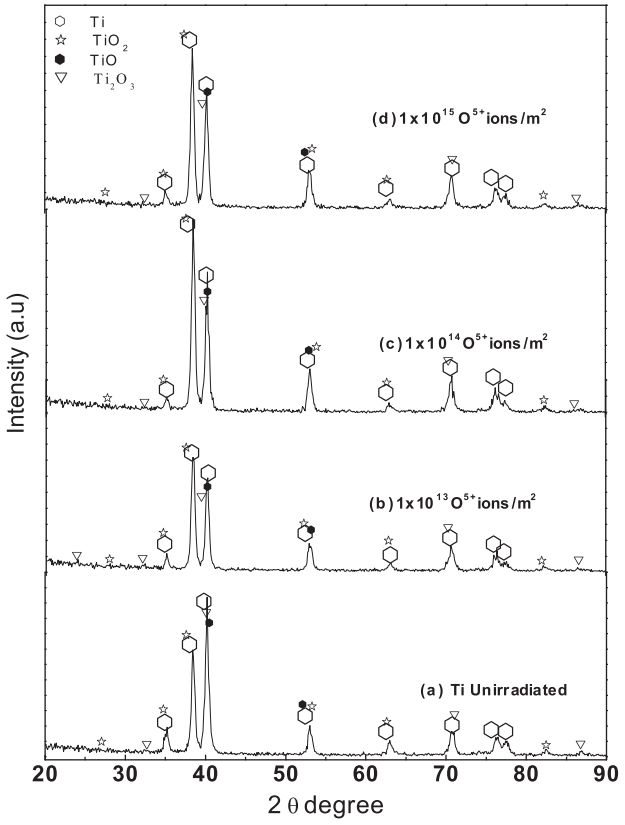

Fig. 2. GXRD profile with and without O^{5+} ion irradiation: (a) Ti unimplated (b) 1×10^{13} ions/cm^2 (b) 1×10^{14} ions/cm^2 and (c) 1×10^{15} ions/cm^2.

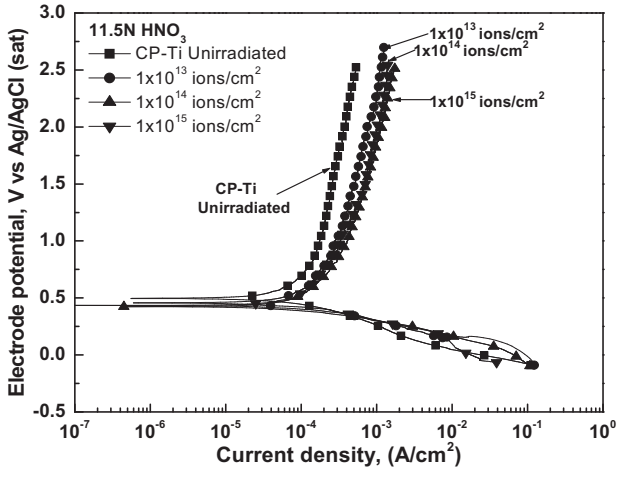

Fig. 3. Potentiodynamic polarization plots measured in 11.5 N HNO_3 in CP-Ti with and without O^{5+} ion irradiation.

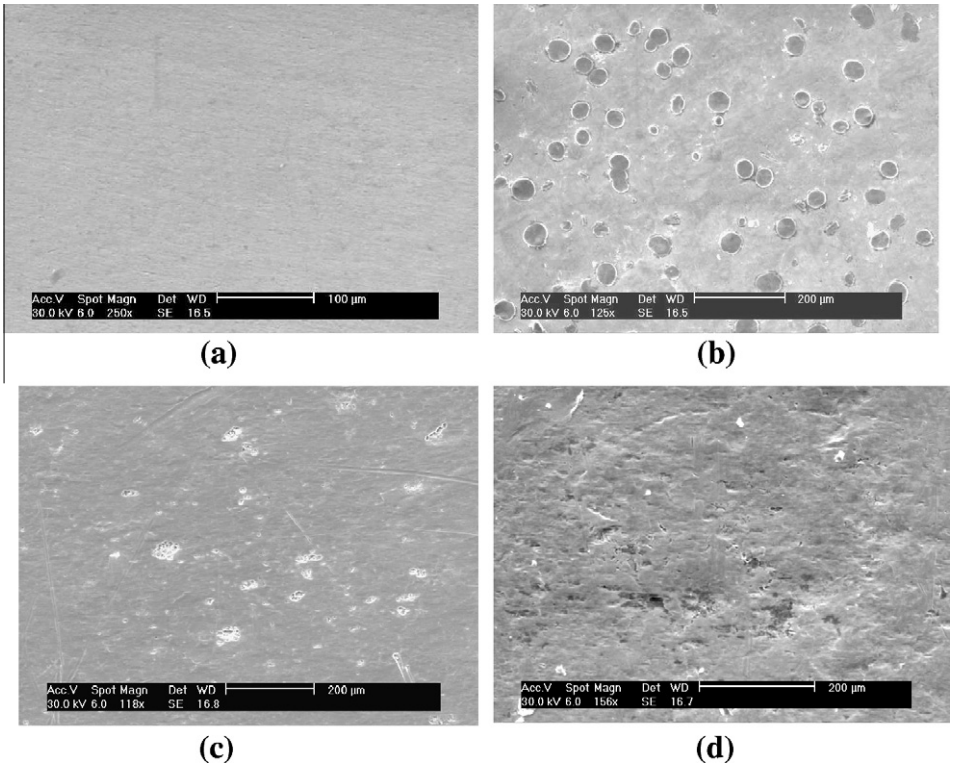

Fig. 4. SEM micrograph; (a) CP-Ti unirradiated specimen (b) O^{5+} ion irradiation fluence of 1×10^{13} ions/cm^2 (c) 1×10^{14} ions/cm^2 Ti and (d) 1×10^{15} ions/cm^2 after corrosion test.

Table 2
Potentiodynamic polarization parameters obtained in 11.5 N HNO_3 solution of CP-Ti with and without O^{5+} ion irradiation (I_{Pass} were measured at 1.5 V).

Alloy (ion dose)	E_{Corr} (V)	I_{Corr} (A/cm^2)	I_{Pass} (A/cm^2)
Unimplanted	0.491	2.27×10^{-4}	0.00025
1×10^{13} ions/m^2	0.455	4.23×10^{-4}	0.00051
1×10^{14} ions/m^2	0.423	3.86×10^{-4}	0.00071
1×10^{15} ions/m^2	0.435	3.25×10^{-4}	0.00070

characteristic trend in E_{Corr} could be observed (Table 2) but marginal increase in I_{Corr} after irradiation was observed. Comparing between with and without irradiation (Fig. 2 and Table 2), increase in ion fluences increased the I_{Pass}. In general, I_{Pass} is a measure of the anodic dissolution or reaction rate at a certain potential in the passive region and it can be used as a measure of the resistance against electrochemical corrosion [2,12]. The increase in I_{Pass} is associated with increase in anodic dissolution [2] and thereby these results revealed deterioration in corrosion resistance by irradiation in CP-Ti. In Ti and its alloys higher passive current density ($\approx 10^{-3}$ A/cm^2) in nitric acid has also been reported [24–26]. Moreover, higher value of I_{Pass} could be attributed to less stability and less protective nature of the passive film and due to the formation of unstable hydrated TiO_2 film or TiO_3, as reported by Kiuchi [8,11]. Further the increase in I_{Pass} by the irradiation can be associated with the reduction of nitric acid that catalyzes the reduction reaction during polarization [2,3,10]. Similarly, improvement in corrosion resistance by oxygen implantation due to oxygen ion induced nanocrystalline rutile TiO_2 formation has been reported by others [27,28]. However, in the present study decrease in corrosion resistance was observed in CP-Ti and this is corroborated by SEM micrographs after corrosion test as shown in Fig. 4a–d. The micrograph before irradiation shows no damage in the surface morphology (Fig. 4a). However, after irradiation at different fluences of 1×10^{13} (Fig. 4b), 1×10^{14} (Fig. 4c) and 1×10^{15} (Fig. 4d), globular like pit attacks (Fig. 4b) and irradiation damage after corrosion were clearly observed (Fig. 4d). Similarly, as observed in GXRD results (Fig. 2), in CP-Ti the ion irradiation introduce a change in TiO_2 profile showing decreased intensity. This revealed that ion irradiation introduces changes not only in the oxide film but also induced irradiation damages in CP-Ti which thereby affect its corrosion resistance. It is well known that the effect of irradiation is strongly depth-dependent and the nature of irradiation damage in the materials is dependent on type of ions used, alloying elements and the impurity variations [18,29]. In case of the light ions ($\geqslant$ 6 MeV) such as protons and deuterons, irradiation damage resulting from atomic displacements by elastic collisions resulted into insignificant surface damage. On the other hand, oxygen being a heavy ion is known to produce displacement cascades, consisting of highly localized interstitials and vacancies [15,29,30]. It has also been reported that in pure Ti [15], dislocation density increased significantly with increase in irradiation fluence. But, the deformation (stacking) fault probabilities were found to be insignificant even in high oxygen fluence of irradiation. The measured damage profile as a function of depth in terms of displacements per atom (dpa) of 116 MeV O^{5+} ion for CP-Ti obtained by TRIM 95 calculation is 78 μm [15]. Sizmann [31] reported that irradiation with high energy particles enhanced diffusion process, defect concentrations and creates different defect species. In particular, irradiation-induced changes in microstructure and microchemistry are major concerns and it has been reported that high radiation fields are known to accelerate corrosion due to enhance hydrogen uptake, permeation, and deposition of spallation products [32]. Yamamoto et al. [33] observe increased in corrosion rate by γ-irradiation in 304L SS while improvement in corrosion resistance was observed in Ti and Ti-5% Ta alloy in 9 N HNO_3. Nitric acid enhancing the passivity and the corrosion rate by a factor of 2–3% in tantalum under radioactive condition has also been reported [34]. Further, since

the radiation induced defects would influence the migration of carriers such as electrons or ions through the passive films on the surface of the materials [16,34] which thereby can affect corrosion. Elfanthal et al. [16] observed increase in defects, dielectric constant and electronic conductivity of passive film in Ti by irradiation. However, the effect of electronic energy deposition and displacements of atoms has not been correlated with corrosion resistance in this study. But, the decrease in corrosion resistance was observed with increase in ion fluences in the presence case, may be attributed to highly oxidizing environment of 11.5 N nitric acid used in the present study which thereby modified the surface and oxide layer by irradiation. Moreover, as only limited studies and information are available for corrosion of CP-Ti in highly oxidizing nitric acid media, further studies will be required to clarify the correlation between ion irradiation and corrosion resistance.

3.3. Irradiation effects on electrochemical impedance characteristic of CP-Ti

In order to investigate the effects of ion irradiation on the passive film properties, EIS measurements were performed on CP-Ti in aerated 11.5 N HNO_3. All the EIS measurement was carried out after stabilizing the open circuit potential (OCP) and the typical Nyquist plots measured in 11.5 N HNO_3 is shown in Fig. 5. The OCP here is referred to potential of an electrode measured with respect to a reference electrode under stabilized equilibrium condition with no external applied current or potential. As can be observed, all the Nyquist plots revealed only one time constant of an unfinished semi-circle arc and distinct differences in the impedance spectra are observed depending on ion irradiated fluences. All the fitting parameters of the impedance plots of CP-Ti are listed in Table 3.

In CP-Ti as shown in Fig. 5, with increase in ion fluences from 1×10^{13} ions/cm^2 to 1×10^{15} ion/cm^2 decrease in semi-circle radius was observed. The increase in semi-circle is associated with increase in polarization resistance (R_P) and the R_P values are strongly dependent on the passive film characteristic and are a measure of corrosion resistance of the materials. The present result revealed that the oxide film stability and thereby corrosion resistance decreased by ion irradiation. As shown in Table 3, higher R_P value for unirradiated CP-Ti implies better corrosion resistance. The decrease in the R_P by increase in ion irradiation fluence could also be due to structural (stoichiometric) changes in the oxide phases as revealed in GXRD results (Fig. 2), which thereby influence the electrochemical corrosion behavior of CP-Ti. In CP-Ti, depending on the nitric concentration and temperature Ti^{4+} ions produced during corrosion processes enhanced passivation by self inhibiting effect leading to formation of TiO_2 and enhanced corrosion resistance [1,9,10]. Beyond 8–10 N HNO_3, the unstable oxide films formed are known to lower the self inhibiting effect of Ti^{4+} ions [7,8,10]. Moreover, the oxide film formed in titanium surface has duplex structure: thinner and compact inner layer and thicker and more porous outer layer [13]. It is likely that such oxide structures will be modified with increase in porosity and non-uniformity by increase in ion irradiation fluence. Besides, the process of ion irradiation can introduce other contaminants that may lower its anti-corrosion ability. The reduction of R_P by ion irradiation may also be correlated with the irradiation damage induced on the metal surface (Fig. 4b–d). Further, due to complexity of metal dissolution process involved in nitric acid corrosion, different metals are known to exhibit different rates of dissolution under comparable experimental conditions [2,35]. In addition, since autocatalytic metal dissolution mechanism are involved in nitric acid corrosion [2,3,11] dissolution will proceed at higher rates in higher nitric acid concentration and thus lower passive film resistance will be observed.

Table 3
EIS fitted value of CP-Ti measured at OCP in 11.5 N HNO_3.

Material condition	R_s (Ω cm^2)	R_p (Ω cm^2)	CPE-T (F/cm^2 s^{-n})	CPE-n
Unimplanted	1.83	637	1.35×10^{-4}	0.831
1×10^{13}	0.55	580	2.58×10^{-4}	0.805
1×10^{14}	1.67	485	4.16×10^{-4}	0.861
1×10^{15}	1.77	352	6.16×10^{-4}	0.876

The measured capacitive responses are generally not ideal in real electrochemical processes, thus CPE is used in the present study to understand the non ideal capacitance of the passive film formed. As shown in Table 3, the Z_{CPE} of T values (Eq. (1)) are relatively lower for unirradiated CP-Ti specimen compared to ion irradiated CP-Ti specimen. Increased T values (capacitance) by ion irradiation could be attributed to the non-homogenous nature of the passive film that deteriorates the protective property of passive film. Lower value of T of unirradiated CP-Ti samples revealed the amount of charge associated with the degree of oxidation of the sample. Hence smaller the charge, higher is the protective nature of the film with more resistance to oxidation and corrosion [12,16]. The power index value of CPE-n (Table 3), which reflected the deviation of capacitance of the passive film from the ideal capacitive behavior, was in the range ≈0.8. These values revealed that the deviation from purely capacitive behavior was relatively small for both the unirradiated and irradiated samples and no characteristic trend in CPE-n value can be observed.

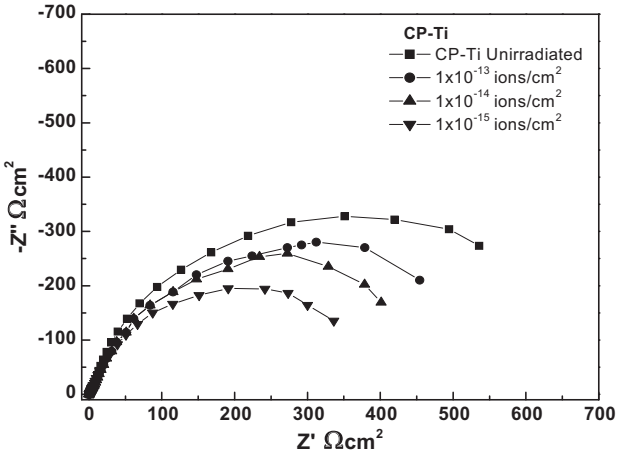

Fig. 5. Nyquist plots measured in 11.5 N HNO_3 in CP-Ti with and without O^{5+} ion irradiation.

4. Conclusions

The O^{5+} ion irradiation effects on corrosion behavior of CP-Ti in aggressive 11.5 N HNO_3 have been studied. The results of GXRD patterns of CP-Ti revealed that the passive oxides are modified by ion irradiation. The potentiodynamic polarization results of CP-Ti revealed increase in passive current density with increase in ion irradiation fluences, thereby revealing decrease in corrosion resistance. SEM micrographs corroborated with these results showing corrosion attack around surrounding matrix with different morphology. The passive film properties studied by EIS indicated a distinct difference in the impedance spectra as indicated by lower film resistance with increase in ion irradiation fluences. Thus, O^{5+} ion irradiation at increasing fluences lowers the corrosion resistance of CP-Ti in highly aggressive 11.5 N HNO_3 solution.

References

[1] Baldev Raj, U. Kamachi Mudali, Prog. Nucl. Energ. 48 (2006) 283.
[2] S. Ningshen, U. Kamachi Mudali, G. Amarendra, Baldev Raj, Corros. Sci. 51 (2009) 322.
[3] P. Fauvet, F. Balbaud, R. Robin, Q.-T. Tran, A. Mugnier, D. Espinoux, J. Nucl. Mater. 375 (2008) 52.
[4] R.D. Armstrong, G.E. Cleland, G.O.H. Whillock, J. Appl. Electrochem. 28 (1998) 1205.
[5] V. Kain, S.S. Shinde, H.S. Gadiyar, Mater. Eng. Perform. 3 (1994) 699.
[6] IAEA-TECDOC-421, Proceedings of a Technical Committee Meeting on Materials Reliability in the Back End of the Nuclear Fuel Cycle, International Atomic Energy Agency, Vienna, Austria, 1987, p. 107.
[7] T. Fujii, H. Baba, Corros. Sci. 31 (1990) 275.
[8] K. Kiuchi, M. Hayashi, H. Hayakawa, M. Sakairi, M. Kikuchi, Proceedings of the Third International Conference on Nuclear fuel Reprocessing and Waste Management (RECOD-91), Sendai, Japan, 14–18 April, 1991, vol. 1, p. 549.
[9] K. Kapoor, Vivekanand Kain, T. Gopalakrishna, T. Sanyal, P.K. De, J. Nucl. Mater. 322 (2003) 36.
[10] A. Robin, J.L. Rosa, H.R.Z. Sandim, J. Appl. Electrochem. 31 (2001) 455.
[11] K. Kiuchi, H. Hayakawa, Y. Takagi, M. Kikuchi, Proceedings of the 4th International Conference on Nuclear fuel Reprocessing and Waste Management (RECOD-94), vol. 3, London, UK, 1994.
[12] S. Ningshen, U. Kamachi Mudali, P. Mukherjee, A. Sarkar, P. Barat, N. Padhy, Baldev Raj, Corros. Sci. 50 (2008) 2124.
[13] A. Takamura, K. Arakawa, Y. Moriguchi, in: R.I. Jaffee, N.E. Promisel (Eds.), The Science, Technology and Application of Titanium, Pergamon Press, Oxford, 1970, p. 209.
[14] B.D. Craig, D.S. Anderson (Eds.), ASM Handbook of Corros. Data, second ed., ASM Publication, Materials Park, OH, USA, 1995. 543.
[15] P. Mukerjee, A. Sarkar, P. Barat, Raj Baldev, U. Kamachi Mudali, Met. Mat. Trans. A 36 (2005) 2351.
[16] L. Elfenthal, J.W. Schultze, Corros. Sci. 29 (1989) 343.
[17] M. Griffiths, D. Faulkner, R.C. Styles, J. Nucl. Mat. 119 (1983) 189.
[18] M. Griffiths, J. Nucl. Mater. 159 (1988) 90.
[19] L.K. Mansur, A.F. Rowcliffe, R.K. Nanstad, S.J. Zinkle, W.R. Corwin, R.E. Stoller, J. Nucl. Mater 329–333 (2004) 166.
[20] M. Drogowska, H. Ménard, A. Lasia, L. Brossard, J. Appl. Electrochem. 26 (1996) 1169.
[21] C.H. Hsu, F. Mansfeld, Corrosion 57 (2001) 747.
[22] A. Pér ez del Pino, P. Serra, J.L. Morenza, Thin Solid Films 415 (2002) 201.
[23] Y. Okabe, M. Iwaki, K. Takahashi, Nucl. Instrum. Methods Phys. Res. 861 (1991) 44.
[24] A. Robin, H.R.Z. Sandim, J.L. Rosa, Corros. Sci. 41 (1999) 1333.
[25] S.Y. Yu, J.R. Scully, Corrosion 53 (1997) 965.
[26] A. Fossati, F. Borgioli, E. Galvanetto, T. Bacci, Corros. Sci. 46 (2004) 917.
[27] D. Krupa, J. Baszkiewicz, J. Kozubowski, A. Barcz, G. Gawlik, J. Jagielski, B. Larisch, Surf. Coat. Technol. 96 (1997) 223.
[28] T. Sawase, A. Wennerberg, K. Baba, Y. Tsuboi, L. Sennerby, C.B. Johansson, T. Albrektsson, Clin. Implant Dentistry Relat. Res. 3 (2001) 221.
[29] L.K. Mansur, K. Farrell, J. Nucl. Mater. 244 (1997) 212.
[30] C. Abromeit, J. Nucl. Mater. 216 (1994) 78.
[31] R. Sizzmann, J. Nucl. Mater. 69–70 (1978) 386.
[32] R.L. Sindelar, P.S. Lam, M.R. Louthan Jr., N.C. Iyer, Mater. Charact. 43 (1999) 47.
[33] T. Yamamoto, S. Tsukui, S. Okamoto, T. Nagai, M. Takeuchi, S. Takeda, Y. Tanaka, J. Nucl. Mater. 228 (1996) 62.
[34] J. Vehlow, Int. J. Appl. Radiat. Isot. 35 (1984).
[35] S.M. Repinskii, Russ. J. Phys. Chem. 37 (1963) 979.